MODELISATION NUMERIQUE DE LA REMISE EN SUSPENSION D'AEROSOLS A L'ECHELLE D'UNE PARTICULE

N.A. Duthou*[1] et A.M. Gambaruto[1]

[1]School of Engineering Mathematics and Technology, University of Bristol, BS8 1QU Bristol, United Kingdom
*Courriel de l'orateur : nicolas.duthou@bristol.ac.uk

TITLE

Numerical Modelling of Aerosol Resuspension at the Single-Particle Scale

RESUME

Un modèle numérique a été développé pour étudier la remise en suspension d'aérosols à l'échelle d'une particule. Il associe un solveur aux volumes finis pour l'écoulement à une description lagrangienne à six degrés de liberté, permettant de représenter les interactions proche paroi et le couplage fluide-particule. Une approche de simulation par courants tourbillonnaires détachés (DES) est employée pour modéliser les phénomènes d'écoulement instationnaires aux nombres de Reynolds typiques lors de la remise en suspension. Les forces adhésives sont intégrées via une formulation de van der Waals adaptée à STAR-CCM+ grâce à une méthode de compensation permettant d'appliquer des forces tensiles et des moments résistants. Des tests de vérification ont été menés sur le modèle de contact et l'intégration des forces adhésives pour garantir un comportement stable et des seuils de décollement cohérents. Les premiers résultats illustrent l'influence de l'intensité de l'écoulement sur les phases de bascule, de soulèvement et de remise en suspension. Ce cadre servira à des validations en soufflerie et à l'étude de morphologies de surface et conditions environnementales plus complexes.

ABSTRACT

A computational model was developed to study aerosol resuspension at the scale of a single particle. It combines a finite-volume flow solver with a six-degree-of-freedom Lagrangian description of particle motion, allowing near-wall dynamics and fluid-particle coupling to be resolved. A Detached Eddy Simulation (DES) approach is used to capture unsteady flow features at relevant Reynolds numbers. Adhesive interactions are included through a van der Waals formulation adapted to STAR-CCM+ via a compensation-based method that allows tensile forces and resisting moments to be applied. Verification tests were carried out on the contact model and adhesive force integration to ensure stable collision behaviour and consistent detachment thresholds. Preliminary results show how flow intensity governs rocking, lifting and resuspension events. The framework is intended to support later validation against wind-tunnel data and to explore more complex surface topologies and environmental conditions.

MOTS-CLES : remise en suspension d'aérosols, mécanique des fluides, modélisation CFD, forces d'adhésion /
KEYWORDS: aerosol resuspension, fluid dynamics, CFD modelling, adhesive forces

1. INTRODUCTION

Aerosol resuspension refers to the process by which particles detach from a surface and become airborne due to the action of external forces (Hinds, 1999). It is a critical yet underexplored source of aerosols in the atmosphere, and often has hazardous implications as it contributes to air quality deterioration and poses exposure risks for people. It is an ubiquitous phenomenon and includes natural instances with sand, sediments and pollens resuspended by the wind; industrial occurrences with dust, fibres and pollutants being moved around through processes or sometimes accidents; medical applications with biological organisms re-entrained by pedestrian movement, ventilation and air conditioning systems; agricultural instances in the delivery of pesticides and fertilisers and transport episodes with worn-out road, track, tyre and brake particles lifted from vehicle motions. All these applications are spatially and temporally diverse, yet some of them are hazardous, if not harmful, when direct exposure occurs. Being able to accurately model and predict resuspension behaviour is thus essential from a health and safety perspective.

Despite its omnipresence across various fields, resuspension is often underrepresented and understudied compared to the likes of aerosol transport and dispersion due to its intrinsic complexity. For resuspension to occur, the particle's dynamic equilibrium needs to be disrupted with removal forces and torques exceeding their adhesive counterparts in magnitude. Removal forces are made of anything trying to induce particle motion. They are very diverse in their nature, as they comprise unsteady fluid dynamics, mechanical forces, electrostatics or even particle impaction. On the other hand, adhesive forces resist the particle motion, and mainly include van der Waals forces (vdW), electrostatics, capillary effects, friction and gravity. The main difficulty behind resuspension modelling is the ability to quantify these forces for every scenario of interest, as they result from four intrinsically coupled characteristic sets: particle properties, surface topology, flow conditions and environment.

Various models have been created since the late 1980s and can mainly be classified as mechanistic, stochastic, probabilistic or empirical. Most of them rely on several assumptions, which can be quite restrictive and may reduce accuracy to lower computational effort and keep calculations simple. The "*Rock'N'Roll*" (RnR) model is a reference in the field; it looks at particles rocking about an asperity and outputs a resuspension rate

DOI : 10.25576/ASFERA-CFA2026-50150

p over time (Reeks et al., 2001; Biasi, 2001). In its original form, some of the main assumptions include semi-empirical/experimental force relations, particle sphericity, limited contact points, vdW force dominance and resuspension induced after rolling occurs, though later works revisited some of these to extend them further (Vincent et al., 2019). Although current models may often be sufficient to investigate a resuspension scenario and evaluate the behaviour of an aerosol population, the assumptions might be inadequate if too simplistic, and confidence insufficient for hazardous cases. Therefore, the purpose of my work is to look at novel ways to model resuspension with a thorough focus on near-wall physics, complex particle/surface morphologies and realistic adhesive forces and contact resolution.

2. NUMERICAL MODEL AND SET-UP

A key requirement for understanding the dynamics of aerosol resuspension is an accurate representation of the flow field around the particle, since fluid motion and aerodynamic characteristics have a strong influence on its detachment. Siemens *Simcenter STAR-CCM+ v2502* was used to perform three-dimensional CFD simulations based on a finite-volume solution to the flow-governing equations. Instead of studying a population of aerosols, a Lagrangian framework is used to resolve translation, rotation and forces at the particle level. For resuspension needs, a Detached Eddy Simulation (DES) approach was employed. It is a hybrid method blending Reynolds-Averaged Navier-Stokes (RANS) treatment in near-wall regions, and Large Eddy Simulations (LES) equations for the far-field flow. For an incompressible, Newtonian fluid (constant viscosity and density), the continuity (1) and momentum (2) equations are given by:

$$\nabla \cdot \boldsymbol{u} = 0 \quad (1) \qquad \rho\left(\frac{\partial \boldsymbol{u}}{\partial t} + \boldsymbol{u} \cdot \nabla \boldsymbol{u}\right) = -\nabla \mathrm{p} + \mu \nabla^2 \boldsymbol{u} + \boldsymbol{F} \quad (2)$$

where **u** is the velocity field, p the pressure, ρ the density, μ the dynamic viscosity and **F** the external forces.

The initial target scenario to model is a representation of the aerosol wind tunnel set-up developed by Neal et al. (2024) to ease the validation process. As such, similar particle sizes and shapes are used, as well as relevant free-stream flow velocities. In preliminary cases, 25.6 and 50 µm-diameter glass spherical particles are resting on a flat surface within a rectangular computational domain. Later simulations will look at smaller particles, with Reynolds numbers Re < 1, in the Stokes regime. The surface topology and particle morphology can be easily altered to look at scenarios of greater complexity, with some later cases also looking at different surface layouts (flat with a ramp, RnR-like asperities). A trimmed (cube-based) mesh of base size Δx = 10 µm is applied to the domain, with local refinements and prism layers of up to 6.5% of Δx near the particle and ground, resulting in a few hundred thousand cells in a typical simulation. An overset mesh is defined around the aerosol to ensure accurate resolution of the two-way particle-fluid coupling while enabling 6-degrees-of-freedom (DOF) motion freedom through the dynamic fluid-body interaction (DFBI) package.

In terms of boundary conditions, the front, back and top planes of the domain are set as far-field "symmetry planes", the right side as a pressure outlet, and the left side as a velocity inlet. A first approximation of an inflow on a flat plate uses a 1/7th power law (Schlichting, 1968) to simulate the turbulent boundary layer (BL) velocity u(z) of the wind tunnel measurement section from its width w and BL thickness δ(w), described by (3) and (4):

$$\frac{u(z)}{u_\infty} = \left(\frac{z}{\delta}\right)^{1/7} \quad (3) \qquad \delta(w) \approx 0.37\frac{w}{Re^{1/5}} \quad (4)$$

To handle particle-surface contacts, as part of the DFBI package, a dynamic equivalent of a mass-spring-damper contact body coupling was calibrated, essentially offsetting the ground surface with a thin layer dedicated to contact resolution. The contact force comprises a normal (5) and tangential (6) component, which are functions of the elastic k_1, damping k_2, dynamic friction μ_f and tanh k_t coefficients, cell face area a_f, distance between face centroid and contact surface d_f, effective contact range d_0, boundary face normal $\mathbf{n_{bf}}$ and tangential velocity v_t:

$$\boldsymbol{f_n}(d_f) = a_f[k_1(d_0 - d_f) - k_2\dot{d}_f]\boldsymbol{n_{bf}} \quad (5) \qquad \boldsymbol{f_t} = -\mu|\boldsymbol{f_n}|\tanh(k_t\boldsymbol{v_t}) \quad (6)$$

k_1 (7) and k_2 (8) were derived from a non-excited system from the particle mass m_p, frequency ω_n inferred from a contact resolution timestep of 0.1ms, the system was assumed to be critically damped with $\zeta = 1$:

$$k_1 = m_p\omega_n^2/a_f \quad (7) \qquad k_2 = 2\zeta\sqrt{m_pk_1}/a_f \quad (8)$$

To ensure a satisfactory level of resolution for both fluid and dynamic aspects, an implicit segregated flow solver was used with a first-order temporal discretisation scheme comprising a baseline timestep Δt = 1E-6 s and an adaptive timestep based on a mean ($\overline{CFL}$ = 1) and max ($CFL \leq 2$) Courant-Friedrichs-Lewy condition.

The baseline fluid behaviour was verified by comparing predicted forces and flow patterns with well-documented cases of fixed spheres in a freestream, as it is a rather standard test case for separated bluff-body flow. Although the comparison is not a full validation for the resuspension problem, it provides insightful checks to ensure the solver captures key flow features at relevant Reynolds numbers (Re). Further validation against wind-tunnel data is planned at a later stage of the research to assess coupled fluid-particle behaviour in near-wall regions and will be mainly focused on the model set-up rather than the widely-established finite-volume formulation of the incompressible Navier-Stokes equations. The spring-damper contact model was checked separately to ensure that the chosen stiffness and damping coefficients produced stable and pertinent

DOI : 10.25576/ASFERA-CFA2026-50150

collision behaviour. This included simple bounce tests against a rigid wall in quiescent and modest background flow to ensure that the restitution and contact times were consistent with soft-sphere dynamics.

An example displacement of a spherical particle rocking about two asperities ($Ø_L$ = 20 and $Ø_R$ =14 µm) with two velocity fields of different free-stream magnitudes (u_∞) can be seen in Fig. 1. The Reynolds number (Re), Stokes number (StK), approach velocity (U_{app}), upstream ground surface shear stress (τ_w) and shear velocity (u_τ) are also indicated. It shows the need for sufficient airflow velocity to achieve resuspension, with the particle rocking, falling back to the ground and failing to resuspend in the 2 m/s case, while in the 10 m/s case, both lifting and resuspension are observed. The 2 m/s case also highlights one of the limitations of the RnR model in assuming that resuspension occurs after a particle rocks and starts rolling, which is not the case here. It should be noted that this is a pre-adhesion behaviour check, with only gravity acting downwards.

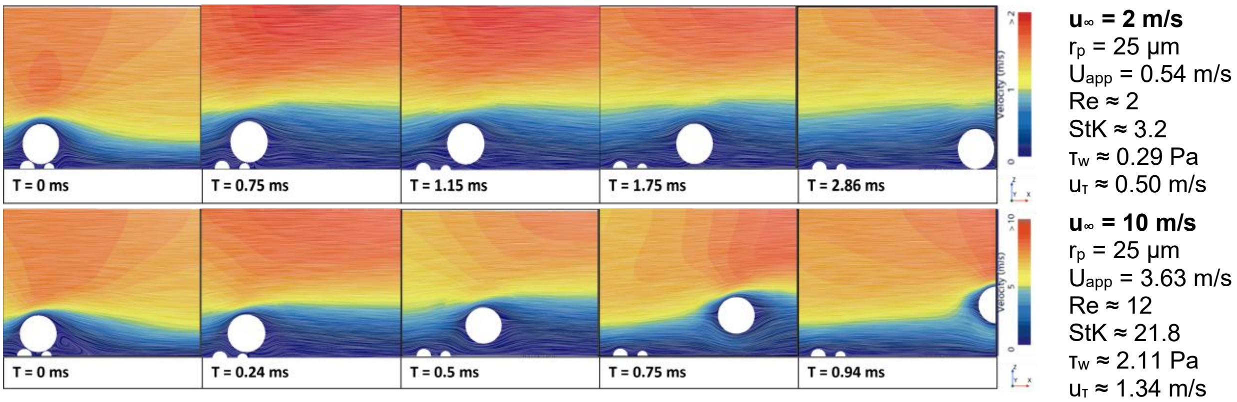

Fig. 1 – Spherical particle rocking about asperities for two different free-stream velocities

3. IMPLEMENTING AND VALIDATING RESUSPENSION-SPECIFIC FORCES

In addition to flow and contact modelling, additional force terms must be included to incorporate real resuspension physics, namely, adhesive forces and torques. The DFBI contact module natively supports compressive force terms, but not tensile ones, so an alternative compensation-based approach was designed. The adhesive force resultant was computed as a function of the shortest path between every point of the domain and its nearest surface node. As the particle moves across the domain, the local force values can be evaluated at all points of the moving body, enabling further calculations of the total adhesive resultant and moment, which need to be overcome for motion and thus resuspension to occur. To ease the implementation and validation processes, only van der Waals (vdW) interactions were considered initially and modelled using a sphere on a flat surface approximation (Israelachvili, 2011):

$$F_{vdW} = -A_H r_p / 6D^2 \qquad (9)$$

where A_H = 6.5E-20J is the Hamaker constant for silica, r_p the particle radius and D the instantaneous particle-surface gap. To avoid singular behaviour when D → 0 µm and account for the maximum mesh refinement available, D_{eff} = max(D,D_{min}) was used with D_{min} = 1 nm. Accounting for additional adhesive terms for electrostatic and capillary effects is a straightforward extension.

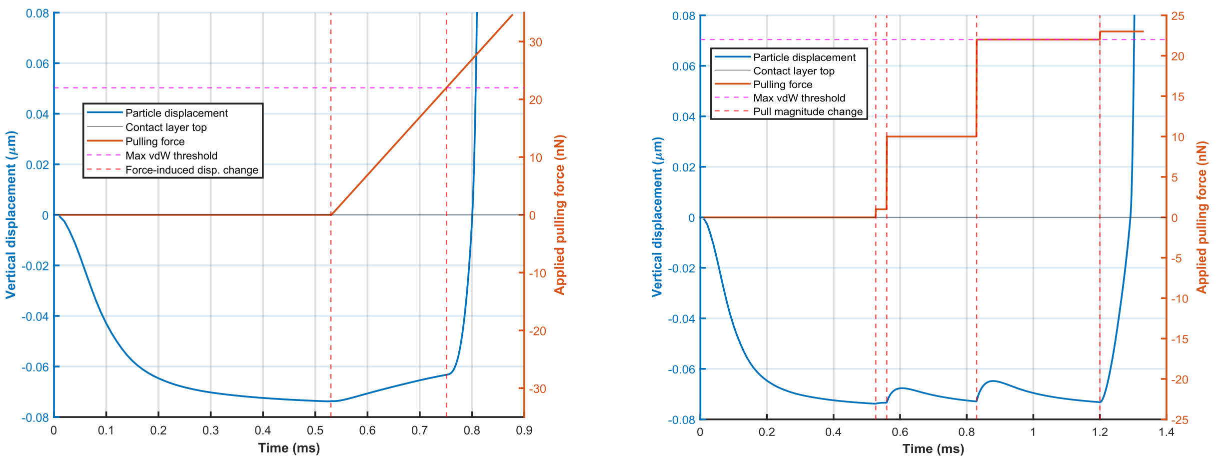

Fig. 2 – Particle vertical displacement Δz induced by transient (left) and step impulse (right) pulling forces

To apply a tensile reaction to a removal force of a compressive nature, all forces acting on the particle ($\Sigma F_{particle}$) are monitored and averaged over a timestep to prevent solver divergence. The magnitude of the resultant is then evaluated and compared to the instantaneous F_{vdW} resultant. If the vdW forces exceed or match the removal forces, vertical motion is prevented by applying a downwards force -|ΣF_{DFBI}|, otherwise only the F_{vdW} term is applied. A limitation of this method is the necessary one-timestep lag, which results in a measurable response delay, which was evaluated below. Multiple cases were thus run to test the solver's behaviour with the delayed application of various types and magnitudes of upwards loads.

Fig. 2 shows the vertical displacement of a particle being initialised on top of the contact resolution layer (z = 0.5 µm when Δz = 0). Initially, the particle sinks into the layer so that $F_{contact}$ = F_g at which point a steady state of rest is achieved. When an upward force is applied onto the particle, the velocity initially increases before force compensation occurs, leading to its decay in subsequent iterations. As a side effect, minimal vertical displacement occurs, but the error tolerance is acceptable with the particle remaining within the contact resolution layer, as Fig. 2 shows. Further mitigation can be done by reducing the timestep if needed. After the pulling force dynamically increases or is set beyond the vdW magnitude, the resultant is capped at a -F_{vdW} and a quick decay occurs with the particle lifting off due to the $1/D^2$ term, as intended.

To compute and apply adhesive moments, the local $F_{vdW,i}$ values at each node i of the particle ($\mathbf{X_{node,i}}$) and their position were stored in an internal table. The adhesive force unit vectors $\mathbf{r_{adh,i}}$ were extracted by taking the gradient of a “distance to surface” field function, which returns the direction of the shortest path towards the surface for each of the particle nodes i. Using Star-CCM+’s Java integration, the moments $\mathbf{M_{adh,i}}$ were calculated about the centre of mass $\mathbf{X_{CoM}}$ in a separate script using eq. (10) to (12):

$$\boldsymbol{r_{CoM,i}} = \boldsymbol{X_{node,i}} - \boldsymbol{X_{CoM}} \quad (10) \qquad \boldsymbol{F_{adh,i}} = F_{vdw,i} \cdot \boldsymbol{r_{adh,i}} \quad (11) \qquad \boldsymbol{M_{adh,i}} = \boldsymbol{r_{CoM,i}} \times \boldsymbol{F_{adh,i}} \quad (12)$$

The resultant three-dimensional moment vector was then used by summing all $\mathbf{M_{adh,i}}$ values across all i nodes. Similar to the forces implementation, the software mainly supports driving moment, so the same method used for tensile forces was also employed to include resisting adhesive moments. This process is triggered at every timestep with a Java workflow to ensure that moments appropriately vary with the evolution of the surroundings of the particle and account for the dynamic motion of its CoM. As this is a recent addition to the model, validation work is still ongoing.

4. CONCLUSION AND FUTURE WORK

STAR-CCM+ was used to set up a three-dimensional, six-degrees-of-freedom Lagrangian resuspension model to investigate a broad range of realistic and industry-relevant scenarios. The model was designed with a high degree of flexibility, combining resuspension physics with a robust CFD pipeline to allow for the implementation of multiple particle morphologies, surface topologies, and turbulent flow boundary profiles. Preliminary cases have been run, with cases illustrating that particles in low-speed flows undergo rocking but remain attached, whereas higher-speed flows produce full detachment. A compensation-based approach was designed to incorporate realistic adhesive torques and forces, and some benchmarking cases were computed to validate the consistency of the adhesive force integration.

Future work includes further model validation through wind tunnel experiments and extensive literature benchmarking. Some sensitivity analysis will be performed with the model, partly through several simulations reproducing realistic industry scenarios. More resuspension aspects, such as particle impaction, multi-layer deposits and the influence of humidity, will also be investigated with the aim of incorporating them in the model.

5. REFERENCES AND ACKNOWLEDGEMENTS

This work was supported by the *EPSRC Centre for Doctoral Training (CDT) in Aerosol Science*, grant reference EP/S023593/1.

Biasi, L. (2001) “Use of a simple model for the interpretation of experimental data on particle resuspension in turbulent flows”, Aerosol Science.

Hinds, W.C. (1999) “Adhesion of particles”, in Aerosol Technology: Properties, Behavior, and Measurement of Airborne Particles, John Wiley & Sons.

Israelachvili, J.N. (2011) “Van der Waals forces between particles and surfaces”, in Intermolecular and Surface Forces, Elsevier. https://doi.org/10.1016/B978-0-12-375182-9.10013-2

Neal, E., Mahato, L.K., Butler, E. et al. (2024) “A novel approach to resuspend particles of controlled morphologies in a 3D printed wind tunnel”, Aerosol Science and Technology, 1–16. https://doi.org/10.1080/02786826.2024.2390669

Reeks, M.W. and Hall, D. (2001) “Kinetic models for particle resuspension in turbulent flows: theory and measurement”, Aerosol Science.

Schlichting, H. (1968) Boundary-Layer Theory, 6th ed., McGraw Hill.

Vincent, J.C., Hill, J., Walker, M.D., Smith, S.A., Smith, S.E. and Cant, N.E. (2019) “Towards a predictive capability for the resuspension of particles through extension and experimental validation of the Biasi implementation of the Rock’n’Roll model”, Journal of Aerosol Science 137, 105435. https://doi.org/10.1016/j.jaerosci.2019.105435